NASA TECHNICAL NOTE

NASA TN D-4267

NASA TN D-4267

THEORETICAL ERROR ANALYSIS OF A DOPPLER RANGE-RATE AND PHASE-MODULATED RANGE TRACKING SYSTEM

by Kenneth J. Bures and Gerald L. Smith

Ames Research Center
Moffett Field, Calif.

NATIONAL AERONAUTICS AND SPACE ADMINISTRATION • WASHINGTON, D. C. • DECEMBER 1967

NASA TN D-4267

THEORETICAL ERROR ANALYSIS OF A DOPPLER RANGE-RATE AND PHASE-MODULATED RANGE TRACKING SYSTEM

By Kenneth J. Bures and Gerald L. Smith

Ames Research Center
Moffett Field, Calif.

NATIONAL AERONAUTICS AND SPACE ADMINISTRATION

For sale by the Clearinghouse for Federal Scientific and Technical Information
Springfield, Virginia 22151 – CFSTI price $3.00

TABLE OF CONTENTS

THEORETICAL ERROR ANALYSIS OF A DOPPLER RANGE-RATE AND PHASE-MODULATED RANGE TRACKING SYSTEM

By Kenneth J. Bures and Gerald L. Smith

Ames Research Center

SUMMARY

A detailed error analysis is presented for a particular type of range and range-rate tracking system. Results are given in the form of analytical expressions for the variances of the various types of errors that affect tracking data. The expressions are written in terms of system parameters so that they can be applied to a wide range of specific systems and tracking situations. The majority of the errors considered are random, but some are bias-like and others are deterministic. The equations given constitute an error model from which data weighting factors can be obtained for use in data processing for the construction of the "best estimate" of the trajectory of a space vehicle.

INTRODUCTION

When data from a tracking system are used to estimate the trajectory of a space vehicle, whether by means of least squares, Kalman filter, or some other method, it is necessary to apply appropriate weighting to each data point to obtain a "best estimate." Since these weights should be proportional to the accuracy of the data, one must have a good idea of the errors that contribute to data inaccuracies. The method of obtaining this information is to perform a detailed error analysis of the equipment, that is, to identify as many of the error sources as possible and, from the known configuration of the system, determine the effects errors from such sources should have upon the data generated in the tracking operation.

This report is concerned with developing, in the above manner, a detailed error model for a hypothetical interrogator-transponder-type sinusoidally phase-modulated range and Doppler range-rate tracking system. The system is assumed to consist of an interrogator aboard a satellite orbiting the moon and a beacon transponder located on the lunar surface. However, the results are equally applicable to the more conventional arrangement of an earth-based interrogator and a space vehicle transponder.

Sinusoidally phase-modulated range and Doppler range-rate systems of the type described here presently find applications in a space vehicle tracking system (refs. 1 and 2), in the SECOR and ANNA geodetic satellites, in the SHIRAN airborne electronic surveying system (ref. 3), and in a zero-zero aircraft landing system (ref. 4). Despite their wide use, it appears that no complete, detailed error analysis has been performed on such range and

range-rate tracking systems. A thorough search of the literature revealed only two previous analyses (refs. 5 and 6), both concerned with the accuracy of the range-rate measurement only. This report considers those errors in both the range and range rate which are listed below:

Range-Rate Errors

1. Master oscillator short-term frequency instability
2. Master oscillator long-term frequency instability
3. Quantization error
4. Phase-locked loop (PLL) error
5. Uncertainty in Doppler averaging time
6. Uncertainty in the speed of light
7. Averaging time error
8. Finite propagation time error

Range Errors

1. Master oscillator short-term frequency instability
2. Master oscillator long-term frequency instability
3. Quantization error
4. Phase-locked loop error
5. Phase detector error
6. Calibration drift errors
7. Uncertainty in the speed of light
8. Finite propagation time error
9. Doppler shift in the ranging tones

Some of these errors are random (i.e., uncorrelated from one data point to the next), some are biases or bias-like, and some are deterministic. In the report these characteristics are pointed out, and formulas for the rms values of each error are developed.

PRINCIPAL SYMBOLS

B	noise equivalent bandwidth of master oscillator phase noise
c	velocity of light
$f(t)$	random frequency component of master oscillator
f_c	range counter pulse generator frequency
f_L	transponder offset frequency
f_{Ld}	one-way Doppler shift of f_L
f_o	bias frequency added to $2f_{td}$
f_t	interrogator transmitter carrier frequency
f_{td}	one-way Doppler shift of f_t
G_r	receiver antenna power gain
G_t	transmitter antenna power gain
$G\varphi(\omega)$	power spectral density of phase fluctuation
k	Boltzmann's constant
$L(\omega)$	second-order PLL transfer function
m	frequency multiplication factor
N	final count of pulse counter
N_R	power spectral density to input of second PLL
N_V	power spectral density to input of first PLL
P	oscillator power
P_r	received power (at antenna)
P_t	radiated (transmitted) power
Q	oscillator selectivity
$\bar{r}$	radius vector to satellite
$\bar{r}_B$	radius vector to beacon
$\bar{R}$	true range

R_m	measured range
$\hat{R}$	estimate of the true range
$\Re$	autocorrelation function
S_L	long-term rms fractional frequency stability, $\Delta f/f$
S_s	short-term rms fractional frequency stability
t	time
t_1	beginning of Doppler counting interval
t_2	end of Doppler counting interval
T	Doppler averaging time
T_c	oscillator coherence time, $2/\Phi$
T^o	temperature, ^oK
$\dot{X},\dot{Y}$	vector components of $\dot{\bar{R}}$
$\dot{X}_a,\dot{Y}_a$	vector components of $\dot{\bar{R}}_a$
$\ddot{X},\ddot{Y}$	vector components of $\ddot{\bar{R}}$
$\Delta\alpha$	elapsed phase angle of carrier during time T
β	beacon latitude
ϵ	phase error in quantization process
ζ	PLL damping ratio
θ	true anomaly of satellite orbit
λ	beacon longitude
λ_m	wavelength of ranging tone
ν	2B
$\bar{\rho}$	component of $\bar{R}$ in orbit plane
σ_{CD}	standard deviation of calibration drift error
σ_P	standard deviation of phase fluctuation
σ_{PD}	standard deviation of phase detector phase error

σ_R	standard deviation of range
$\sigma_{\dot{R}}$	standard deviation of range rate
τ	two-way propagation time, approximated by $2R/c$
$\varphi(t)$	phase angle of noise component of oscillator output
$\varphi_d(t)$	phase angle of Doppler shift frequency
$\varphi_m(t)$	phase angle between received and reference ranging tone
φ_{md}	phase angle of a ranging tone with a Doppler shift
Φ	white power spectral density of $f(t)$
Φ_n	normalized power spectral density of additive white noise at the input of the first PLL
Φ_R	normalized power spectral density of additive white noise at the input of the second PLL
ω_d	PLL damped natural frequency, $\omega_n \sqrt{1 - \zeta^2}$
ω_n	PLL undamped natural frequency

Description of the Range-Rate System

Figure 1 is a block diagram of the range-rate measuring system and figure 2 is a block diagram of the transponder.

The satellite interrogator transmits a signal with carrier frequency f_t. The signal received by the beacon transponder has a frequency of $f_t + f_{td}$, where f_{td} is the one-way Doppler shift due to the relative motion of the beacon and the satellite. The received signal is mixed (fig. 2) with a local oscillator signal of frequency $(m-1)f_L$, where f_L is the local oscillator frequency and m is a frequency multiplication factor, to give an IF signal with frequency $f_t + f_{td} - (m-1)f_L$. The IF signal is amplified and then mixed with another local oscillator signal of frequency mf_L to give a signal with frequency $f_t + f_{td} + f_L$. This signal (an amplified copy of the input signal shifted in frequency by f_L) is further amplified and retransmitted. In addition, a carrier with frequency mf_L is transmitted.

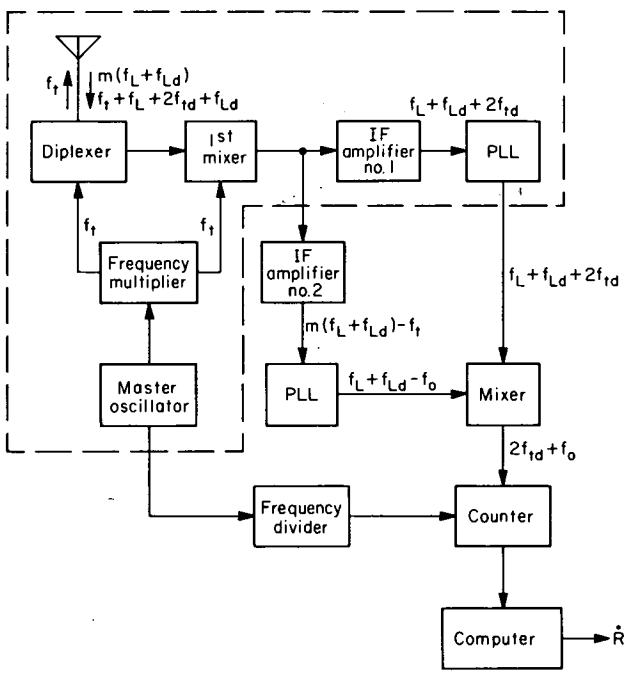

Figure 1.- Range rate system.

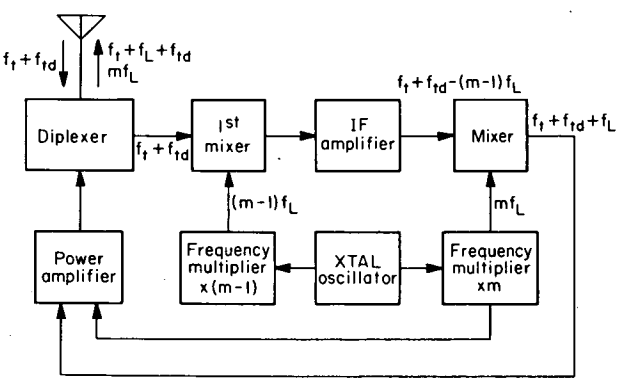

Figure 2.- Transponder.

Because of the relative velocity of the satellite and beacon, the transponder signals are received at the satellite with frequencies $f_t + f_L + 2f_{td} + f_{Ld}$ and $m(f_L + f_{Ld})$, respectively, where f_{Ld} is the one-way Doppler shift in the transponder local oscillator signal. The received signal is mixed with the interrogator transmitter signal producing sum and difference frequencies $f_L + 2f_{td} + f_{Ld}$, $2f_t + f_L + 2f_{td} + f_{Ld}$, and $m(f_L + f_{Ld}) \pm f_t$ (see fig. 1). Number 1 IF amplifier passes only the signal with frequency $f_L + f_{Ld} + 2f_{td}$, and number 2 IF amplifier passes only the $m(f_L + f_{Ld}) - f_t$ signal. Through a series of signal manipulations, represented in figure 1 as simply PLL (phase-locked loop) but described in detail in reference 1, signals with frequencies $f_L + f_{Ld} + 2f_{td}$ and $f_L + f_{Ld} - f_o$, where f_o is a known bias frequency, are obtained. These are mixed together and low-pass filtered to yield a signal with

frequency $2f_{td} + f_o$, which is just the two-way Doppler shift of the interrogator carrier plus a known bias frequency.

This frequency is measured by counting the number of zero crossings of the Doppler waveform in a given interval of time determined by the master oscillator. The count is related to the two-way Doppler shift; therefore, the range rate can be obtained in the computer by the relationship between range rate and Doppler frequency shift. That relationship, derived in appendix A, is

$$\dot{R} = \frac{cf_{td}}{f_t} \tag{1}$$

where $\dot{R}$ is the range rate and the two-way Doppler frequency shift is $2f_{td}$.

Stochastic Errors

Master oscillator short-term[1] frequency instability.- If the transmitter signal of frequency f_t drifts by an amount Δf_t during the roundtrip propagation time, then on reception the apparent Doppler shift will be $2f_{td} + \Delta f_t$. The Δf_t is interpreted as part of the two-way Doppler shift and hence an error in the range-rate measurement occurs.

Suppose the transmitted signal has a frequency $f_t + f(t)$ where $f(t)$ is a zero mean time-stationary random frequency fluctuation. Then the signal received by the interrogator is of frequency $f_t + f_L + 2f_{td} + f_{Ld} + f(t-\tau)$, where τ is the two-way propagation time. The output of the first mixer is equal to the difference frequency $f_L + f_{Ld} + 2f_{td} + f(t-\tau) - f(t)$. After several stages of signal processing as described previously, the offset frequency f_L and its associated Doppler shift f_{Ld} are removed and a bias frequency f_o is added. The bias frequency serves as a convenience in the cycle counting process and is removed in the computer. Therefore, the following analysis is not affected if this term is neglected and the input to the counter is considered to have a frequency $2f_{td} + f(t-\tau) - f(t)$. Associated with this frequency is a phase angle $\varphi_d + \varphi(t-\tau) - \varphi(t)$.

The cycle counting process, in effect, measures the elapsed phase angle $\Delta\alpha$ of the input signal during the time interval $t_2 - t_1 = T$, where t_1 and t_2 are the times at the beginning and end of the counting interval. The average frequency is

$$\frac{\Delta\alpha}{T} = \frac{1}{T}\left[\varphi_d(t_2) + \varphi(t_2 - \tau_2) - \varphi(t_2) - \varphi_d(t_1) - \varphi(t_1 - \tau_1) + \varphi(t_1)\right] \tag{2}$$

---

[1]In this report, "short-term" means time durations comparable to the two-way propagation time τ.

This average frequency is interpreted as the Doppler shift frequency and, therefore, can be substituted for $2f_{td}$ in equation (1) to yield the apparent average range rate over period T:

$$\dot{R} = \frac{c\,\Delta\varphi_d}{2\omega_t T} - \frac{c}{2\omega_t T}\left[\varphi(t_2) - \varphi(t_2 - \tau_2) - \varphi(t_1) + \varphi(t_1 - \tau_1)\right] \tag{3}$$

The second term of equation (3) is the range-rate error due to oscillator instability. The rms value of this error is

$$\sigma_{\dot{R}} = \frac{c}{2\omega_t T}\left(\overline{\left\{\left[\varphi(t_2) - \varphi(t_1)\right] - \left[\varphi(t_2 - \tau_2) - \varphi(t_1 - \tau_1)\right]\right\}^2}\right)^{1/2} \tag{4}$$

where the bar means "average." Equation (4) can be expanded within the brackets to yield

$$\sigma_{\dot{R}} = \frac{c}{2\omega_t T}\left\{\overline{\left[\varphi(t_2) - \varphi(t_1)\right]^2} - 2\overline{\left[\varphi(t_2) - \varphi(t_1)\right]\left[\varphi(t_2 - \tau_2) - \varphi(t_1 - \tau_1)\right]} + \overline{\left[\varphi(t_2 - \tau_2) - \varphi(t_1 - \tau_1)\right]^2}\right\}^{1/2} \tag{5}$$

The averaging time T is normally kept small enough so that $\tau_1 = \tau_2 = \tau$. Using this approximation and noting that $t_2 = t_1 + T$ we see that

$$\varphi(t_2) - \varphi(t_1) = \varphi(t_1 + T) - \varphi(t_1) \tag{6}$$

and

$$\varphi(t_2 - \tau_2) - \varphi(t_1 - \tau_1) = \varphi\left[(t_1 - \tau) + T\right] - \varphi(t_1 - \tau) \tag{7}$$

Equation (6) represents the phase <u>difference</u> in the Doppler signal between time t_1 and t_2, an interval of T seconds. Equation (7) also represents the phase <u>difference</u> which occurs in an interval of T seconds; but in this case, the interval T is shifted by τ seconds with respect to that of equation (6). Therefore, the first and last terms in the brackets in equation (5) are both equal to $R(0)$, the autocorrelation function of the phase <u>difference</u> with a correlation time of zero seconds; and the middle term in the brackets in equation (5) is equal to $2R(\tau)$, twice the autocorrelation function of the phase <u>difference</u> with a correlation time of τ seconds. Therefore, equation (5) can be written as

$$\sigma_{\dot{R}} = \frac{c}{\sqrt{2\omega_t T}} \left[\Re(0) - \Re(\tau) \right]^{1/2} \tag{8}$$

The autocorrelation function $\Re(\tau)$ must now be calculated.

Frequency is defined as the time derivative of phase; therefore, the phase difference $\Delta\varphi$ of equations (6) and (7) can be written in terms of frequency as

$$\Delta\varphi = \int_{t-T}^{T} f(t)dt \tag{9}$$

Integrating by parts yields the Fourier transform of equation (9). From this the power spectral density of the phase difference is found in terms of the power spectral density $\Phi(\omega)$ of the frequency fluctuation $f(t)$. Finally, the inverse Fourier transform yields the autocorrelation function $\Re(\tau)$. (For details, the reader is referred to ref. 5.) When the frequency fluctuation is white noise with a one-sided power spectral density Φ, the autocorrelation function of the phase difference is

$$\Re(\tau) = \begin{cases} \frac{\Phi T}{2}\left(1 - \frac{|\tau|}{T}\right) & 0 \le |\tau| \le T \qquad (10a) \\ 0 & T \le |\tau| \le \infty \qquad (10b) \end{cases}$$

The autocorrelation function $\Re(0)$ is obtained by letting $\tau = 0$ in equation (10). Substituting $\Re(\tau)$ and $\Re(0)$ into equation (8) and letting $2/\Phi = T_c$, the oscillator coherence time,[2] results in an rms range-rate error equal to

$$\sigma_{\dot{R}} = \begin{cases} \frac{c}{\sqrt{2\omega_t T}} \left(\frac{2R}{cT_c}\right)^{1/2} & 0 \le R \le \frac{cT}{2} \qquad (11a) \\ \frac{c}{\sqrt{2\omega_t T}} \left(\frac{T}{T_c}\right)^{1/2} & \frac{cT}{2} \le R \le \infty \qquad (11b) \end{cases}$$

The white noise assumption is, of course, a simplification. Baghdady, Lincoln, and Nelin (ref. 8) have shown theoretically that a more realistic power spectral density for $f(t)$ is

---

[2]Coherence time (ref. 7) is defined as the time required for the rms value of the phase difference between a noisy oscillator and a perfect oscillator to reach one radian.

$$\Phi(\omega) = \frac{a}{\omega} + b + c\omega^2 \tag{12}$$

except for high and very low frequencies. The first term of equation (12) is flicker noise, a low-frequency process caused by current and voltage fluctuations in electron tubes and transistors, by mechanical vibrations, and by temperature variations. The second term of equation (12) is white noise due to thermal noise in the oscillator. Finally, the third term of equation (12) is due to noise associated with certain accessory circuits of the oscillator. Usually, the response of the buffer amplifier following the oscillator falls off faster than $1/\omega^2$ for frequencies greater than half the amplifier bandwidth, so that $\Phi(\omega)$ gradually approaches zero as ω approaches infinity. Equation (12) predicts an infinite power spectral density at $\omega = 0$; however, in practice, $\Phi(\omega)$ levels out rapidly and may even decrease as ω approaches zero (ref. 8). Therefore, $\Phi(\omega)$ is not as dependent on frequency as equation (12) would indicate. This is substantiated experimentally; in fact, Vessot, Mueller, and Vanier (ref. 9) have found that thermal noise is the major factor limiting short-term oscillator stability, particularly with atomic standards.

Equation (11) can be arranged to show the dependence of $\sigma_R^{\cdot}$ on the oscillator short-term stability factor S_s and on the range R by eliminating the coherence time T_c. Substituting Edson's expression of coherence time (ref. 7) in terms of oscillator parameters, namely,

$$T_c = \frac{2PQ^2}{KT^{\circ}\omega_t^2} \tag{13}$$

into his expression for rms fractional phase deviation,

$$\frac{\Delta\varphi}{\varphi} = \sqrt{\frac{KT^{\circ}}{2TPQ^2}} \tag{14}$$

results in an expression for the fractional phase (and, hence, frequency) deviation in terms of coherence time:

$$\frac{\Delta\varphi}{\varphi} = \frac{\Delta f}{f} = S_s = \frac{1}{\omega_t\sqrt{TT_c}} \tag{15}$$

Finally, substituting equation (15) into (11) and letting $\tau = 2R/c$ gives the desired result:

$$\sigma_{\dot{R}} = \begin{cases} S_s\left(\frac{Rc}{T}\right)^{1/2} & 0 \le R \le \frac{cT}{2} \quad (16a) \\ \frac{cS_s}{\sqrt{2}} & \frac{cT}{2} \le R \le \infty \quad (16b) \end{cases}$$

Master oscillator long-term frequency instability.- In addition to the white-noise-type, short-term frequency fluctuations discussed in the previous section, a bias-type error is introduced when the Doppler frequency shift is converted into range rate. Equation (1) shows that the oscillator frequency f_t must be known exactly if the range rate is to be determined correctly. However, since f_t is not precisely known, an error occurs.

The range-rate error is found by differentiating equation (1) with respect to f_t and substituting the derivative into the total differential:

$$\Delta\dot{R} = \frac{\partial\dot{R}}{\partial f_t}\Delta f_t \quad (17)$$

The result is

$$\Delta\dot{R} = \frac{cf_{td}}{f_t}\frac{\Delta f_t}{f_t} = \dot{R}\frac{\Delta f_t}{f_t} \quad (18)$$

If $\Delta f_t/f_t$ is interpreted as the rms uncertainty in f_t, that is, the rms long-term fractional frequency instability S_L, then the rms range-rate error is

$$\sigma_{\dot{R}} = \dot{R}S_L \quad (19)$$

Quantization error.- The process of counting the number of half-cycles of Doppler frequency in a given time T can be viewed as an analog-to-digital conversion of a phase angle. However, the conversion is not exact. The counter has a resolution of only one half-cycle since it counts zero crossings; therefore, the half-cycle count N does not include the portion ϵ shown in figure 3. Because the phase angle ϵ is not included in the count N, the measured frequency is less than the true frequency. All values of ϵ within the bounds $0 < \epsilon < \pi$ are

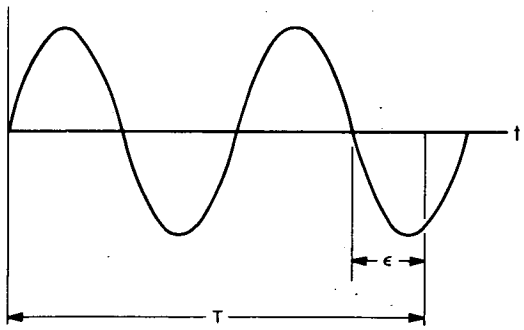

Figure 3.- Quantization error.

possible and equally likely. The maximum error, $\epsilon_{max} = \pi$, results in the maximum count error ΔN_{max} of -1. The count N is equal to

$$N = 2T(f_o + 2f_{td}) \tag{20}$$

The maximum error in Doppler frequency $\Delta f_{td_{max}}$ can be obtained by evaluating the total differential

$$2\,\Delta f_{td_{max}} = \frac{2\,\partial f_{td}}{\partial N}\,\Delta N_{max} = \frac{\Delta N_{max}}{2T} = \frac{1}{2T} \tag{21}$$

where $\partial f_{td}/\partial N$ is obtained from equation (20). The maximum range-rate error $\Delta\dot{R}_{max}$ can be obtained by differentiating equation (1) with respect to f_{td} and substituting the derivative into the total differential:

$$\Delta\dot{R}_{max} = \frac{\partial\dot{R}}{\partial f_{td}}\,\Delta f_{td_{max}} \tag{22}$$

Then, substituting equation (21) into (22) yields an expression for the maximum range-rate error:

$$\Delta\dot{R}_{max} = \frac{c}{4f_tT} \tag{23}$$

Since all ϵ, $0 < \epsilon < \pi$, are equally likely, the probability density function of ϵ is uniform. Therefore, $\Delta\dot{R}$ also has a uniform probability density function with probability $1/\Delta\dot{R}_{max}$ over the interval $0 \leq \Delta\dot{R} \leq \Delta\dot{R}_{max}$. It can be shown that for this rectangular distribution the mean is $\Delta\dot{R}_{max}/2$ and the standard deviation is $\Delta\dot{R}_{max}/2\sqrt{3}$.

The error just considered also appears at the beginning of the counting period. In this case, the error is always such that the frequency reading is greater than the true value and the maximum count error is now $\Delta N_{max} = +1$. The analysis follows exactly as above, with the results that the mean is $-\Delta\dot{R}_{max}/2$ and the standard deviation is $\Delta\dot{R}_{max}/2\sqrt{3}$.

The quantization errors at the beginning and end of the counting period are independent; therefore, their variances add. Thus, the overall quantization error variance is

$$\sigma_{\dot{R}}^2 = 2\,\frac{(\Delta\dot{R}_{max})^2}{12} \tag{24}$$

Substituting equation (23) into (24) gives the rms error in range rate due to quantization:

$$\sigma_{\dot{R}} = \frac{c}{4\sqrt{6}f_t T} \tag{25}$$

Note that the rms range-rate error is not a function of range or range rate; it depends entirely on the digital-to-analog conversion process. The mean quantization error is zero.

Phase-locked loop error.- This section considers the effect of the phase-locked loop (PLL) on the range-rate measurement. The phase-locked loop introduces error in the range-rate measurement in two ways: (1) by the inability of the loop to track the Doppler signal exactly and (2) by the additive noise which corrupts the input signal and is subsequently processed with the signal by the phase-locked loop.

The first error can usually be made negligible by proper design of the loop filter. With a high-order loop filter, the error could theoretically be exactly compensated since the Doppler shift is a more or less deterministic function.

The effect of additive receiver noise cannot be neglected. There are two types of additive noise interferences: thermal (white) noise in the receiver components and external noise sources. In conventional communications systems operating at frequencies above 300 MHz the most important source of noise is the input section of the receiver (electron tubes, transistors, and crystal mixers). However, with receivers employing extremely low noise devices (cooled crystal mixers and masers), the noise attributed to external sources is the limiting factor in receiver performance. The sun and the Milky Way are the two principal external noise sources;[3] of these two, solar noise is several orders of magnitude greater than galactic noise. The solar noise consists essentially of a slowly varying component (sunspot cycle) superimposed on a stationary white noise component. The galactic noise spectrum is not white, but over the relatively narrow bandwidth of the receiver the spectrum is essentially constant (see ref. 10 for further information).

Thus, in the following analysis the noise is assumed to be gaussian white noise, with a constant power spectral density N_V. The value of N_V depends to some extent on the carrier frequency. However, any accurate figures on the noise power must be obtained by actual measurement, or at least by analysis of the particular equipment and mission under consideration. The values given in this paper are typical.

It can be shown by letting $\varphi(t_1 - \tau_1)$ and $\varphi(t_2 - \tau_2)$ in equation (4) equal zero that the rms error in range rate due to phase fluctuations (rather than fluctuations in phase difference as in eq. (4)) is

$$\sigma_{\dot{R}} = \frac{c}{2\omega_t T}\left[\overline{\varphi(t+T)^2} - \overline{2\varphi(t)\varphi(t+T)} + \overline{\varphi(t)^2}\right]^{1/2} \tag{26}$$

---

[3]For an earth-based receiver the earth's atmosphere would also be a noise source.

where the bar means average, and $\varphi(t)$ represents the phase noise due to additive white noise. In terms of autocorrelation functions, equation (26) becomes

$$\sigma_{\dot{R}} = \frac{c}{\sqrt{2}\omega_t T} [\Re(0) - \Re(T)]^{1/2} \tag{27}$$

The autocorrelation function $\Re(T)$ is found by the well-known technique of taking the inverse Fourier transform of the power spectral density of the PLL output. This is written in terms of the closed-loop transfer function $L(\omega)$ and the phase noise normalized power spectral density Φ_n as

$$\Re(T) = \frac{1}{2\pi} \int_{-\infty}^{\infty} |L(\omega)|^2 \Phi_n(\omega) e^{j\omega T} \, d\omega \tag{28}$$

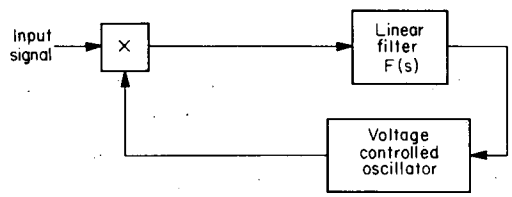

(a) Block diagram.

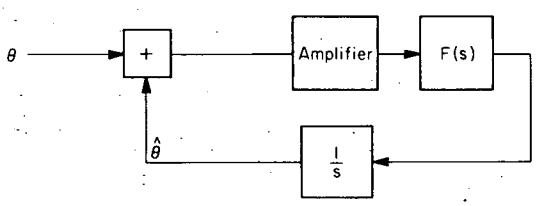

(b) Linear model.

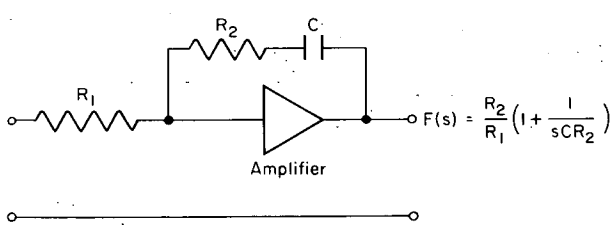

(c) Active linear filter, F(s).

Figure 4.- Phase-Locked Loop (PLL).

A block diagram of the phase-locked loop is shown in figure 4(a) and a linearized model is shown in figure 4(b). For the linear proportional-plus-integrator filter F(s) shown in figure 4(c), the closed-loop transfer function $L(\omega)$ of the PLL is

$$L(\omega) = \frac{\omega_n^2 + j2\zeta\omega_n\omega}{\omega_n^2 + j2\zeta\omega_n\omega - \omega^2} \tag{29}$$

where ω_n is the undamped natural frequency and ζ, the damping ratio of the system. Hence,

$$|L(\omega)|^2 = \frac{1 + \left(\frac{\omega}{\omega_n}\right)^2 4\zeta^2}{\left(\frac{\omega}{\omega_n}\right)^4 + 2(2\zeta^2 - 1)\left(\frac{\omega}{\omega_n}\right) + 1} \tag{30}$$

substituting equation (30) into (28) and integrating using residues (ref. 11)[4] gives

[4]Reference 5 gives $\Re(T)$ for a second-order PLL containing a passive linear filter. Here $\Re(T)$ is presented for a second-order PLL with an active filter because the active filter provides better tracking performance (p. 29, ref. 12).

$$\mathcal{R}(T) = \frac{\Phi_n \omega_n}{8} e^{-\omega_n \zeta T}\left[\frac{\omega_n}{\omega_d}(1 - 4\zeta^2)\sin \omega_d T + \frac{1 + 4\zeta^2}{\zeta}\cos \omega_d T\right] \tag{31}$$

where ω_d is the damped natural frequency $\omega_n\sqrt{1 - \zeta^2}$. The autocorrelation function $\mathcal{R}(0)$ is found by letting $T = 0$ in equation (31)

$$\mathcal{R}(0) = \frac{\Phi_n \omega_n}{8}\frac{1 + 4\zeta^2}{\zeta} \tag{32}$$

Equations (31) and (32) are substituted into equation (27) to give the rms range-rate error due to additive white receiver noise:

$$\sigma_{\dot{R}} = \frac{c\sqrt{\Phi_n \omega_n}}{8\pi f_t T}\left\{\frac{1 + 4\zeta^2}{\zeta} - e^{-\omega_n \zeta T}\left[\frac{\omega_n}{\omega_d}(1 - 4\zeta^2)\sin \omega_d T + \frac{1 + 4\zeta^2}{\zeta}\cos \omega_d T\right]\right\}^{1/2} \tag{33}$$

The normalized power spectral density of the additive white noise is defined as

$$\Phi_n = \frac{\text{Power spectral density of noise}}{\text{Average received signal power}} = \frac{N_V}{P_r} \tag{34}$$

The average received signal power is given by the following equation (ref. 13):

$$P_r = \frac{c^2 G_t G_r P_t}{16\pi^2 K f^2}\frac{1}{R^2} \tag{35}$$

where G_t and G_r are the transmitter and receiver antenna gains, P_t is the transmitted power, and K is a constant which takes into account any receiver gain between the antenna and the input to the PLL. The table below gives the power gain of several representative antenna configurations. (A is the effective area of the antenna.)

TABLE I.- ANTENNA POWER GAINS

Antenna	Power gain
Isotropic	1
Infinitesimal dipole	1.5
Half-wave dipole	1.64
Optimum horn	$10Af_t^2/c^2$
Parabola or lens	$(6.3 \text{ to } 7.5)\ Af_t^2/c^2$
Broadside array	$4Af_t^2/c^2$

Substituting equation (35) into (34) yields

$$\Phi_n = \left(\frac{16\pi^2 K N_V f_t^2}{c^2 G_t G_r P_t}\right) R^2 = K_V R^2 \tag{36}$$

where K_V is equal to the quantity in parentheses in equation (36). Finally, substituting equation (36) into (33) results in an rms range-rate error

$$\sigma_{\dot{R}} = \frac{cR\sqrt{K_V \omega_n}}{8\pi f_t T}\left\{\frac{1 + 4\zeta^2}{\zeta} - e^{-\omega_n \zeta T}\left[\frac{\omega_n}{\omega_d}(1 - 4\zeta^2)\sin \omega_d T + \frac{1 + 4\zeta^2}{\zeta}\cos \omega_d T\right]\right\}^{1/2} \tag{37}$$

Uncertainty in Doppler averaging time.- The Doppler frequency shift is measured by counting the number of half-cycles in a given counting interval T. An error in the counting time will give an error in the measured Doppler frequency and hence in the range rate.

The timing pulses which determine the counting time are generated electronically by division of the master oscillator frequency. The error in T is due to jitter in the frequency dividers and drift in the master oscillator.

The frequency dividers introduce a small time delay between the application of the trigger pulse and the appearance of the output pulse. If the delay were constant, it could be compensated for; however, the effect is a function of transistor and circuit parameter variations, power supply voltage fluctuations, and extraneous signal couplings. All these factors cause a phase jitter to be superimposed on the timing pulse. Normally, the phase jitter is compounded in each stage of a multistage frequency divider. It is possible, however, to design a multistage divider that has the time delay of only one stage (ref. 14). Therefore, by proper design this error can be made negligibly small (on the order of nanoseconds).

A more important jitter source is the master oscillator frequency instability. This error is analyzed by solving equation (20) for f_{td} and substituting the result into equation (1) to give

$$\dot{R} = \frac{cN}{4f_t T} - \frac{cf_o}{2f_t} \tag{38}$$

Equation (38) is differentiated with respect to T and the derivative substituted into the total differential:

$$\Delta\dot{R} = \frac{\partial \dot{R}}{\partial T}\Delta T = \left(\frac{c}{2f_t}\right)\left(\frac{N}{2T}\right)\left(\frac{\Delta T}{T}\right) \tag{39}$$

The quantity N/2T can be obtained from equation (20) and substituted into (39) to give

$$\Delta\dot{R} = \left(\frac{cf_{td}}{f_t} + \frac{cf_o}{2f_t}\right)\frac{\Delta T}{T} \tag{40}$$

The first term in the parentheses of equation (40) is the range rate expressed in equation (1), and $\Delta T/T$ is the oscillator fractional frequency error whose rms value is the oscillator instability S_s. Therefore, the rms range-rate error due to uncertainty in the duration of the counting interval is

$$\sigma_{\dot{R}} = \left(\dot{R} + \frac{cf_o}{2f_t}\right)S_s \tag{41}$$

It should be noted that this error is not correlated with the error of equation (16). The frequency variation $\Delta f/f$ which gives rise to equation (16) is the random frequency change which occurs during the time delay τ between the transmission and reception of the signal, whereas the $\Delta f/f$ which gives rise to equation (41) is the difference between the actual frequency and the assumed (nominal) oscillator frequency during the count period T. These two errors are not the same, hence their effects on the range-rate error are uncorrelated. However, the rms values of both of the error contributions are proportional to the same fractional frequency variance, S_s.

Uncertainty in the speed of light.- It can be seen from equation (1) that the conversion of Doppler shift to range rate requires a knowledge of the velocity of light c. The velocity of light is, however, not known exactly. Reference 15 gives the three-sigma fractional uncertainty $\Delta c/c$ as 10^{-6}. Therefore, the standard deviation of the fractional uncertainty $\Delta c/c$ is 3.33×10^{-7}.

The error in range rate due to the uncertainty in the knowledge of the velocity of light can be found by differentiating equation (1) with respect to c and substituting the result into the total differential:

$$\Delta\dot{R} = \frac{\partial\dot{R}}{\partial c}\Delta c = \frac{f_{td}}{f_t}\Delta c = \frac{cf_{td}}{f_t}\frac{\Delta c}{c} = \dot{R}\frac{\Delta c}{c} \tag{42}$$

Substituting the numerical value of $\Delta c/c$ into (42) gives the standard deviation in range rate due to the uncertainty in the speed of light.

$$\sigma_{\dot{R}} = (3.33 \times 10^{-7})\dot{R} \tag{43}$$

This is a bias-type error.

Deterministic Errors

Averaging time error.- The range rate measured by the Doppler cycle-counting process is an average range rate over a finite averaging time interval T. This average value is equal to the true range rate only at some unknown instant of time in the interval T. Usually, the average range rate is considered to be the true range rate at the middle of the averaging time interval T. Hence, there is an error

$$\Delta\dot{R} = \dot{R} - \dot{R}_a \tag{44}$$

where $\dot{R}_a$ is the average (measured) range rate and $\dot{R}$ is the true range rate at the middle of the interval T. Clearly the averaging time error is dependent on the satellite orbit geometry. An expression is derived in this section assuming a circular orbit. This geometry was selected because it gives the most insight into the problem. The more practical cases of the elliptic and hyperbolic orbits are derived in appendix B.

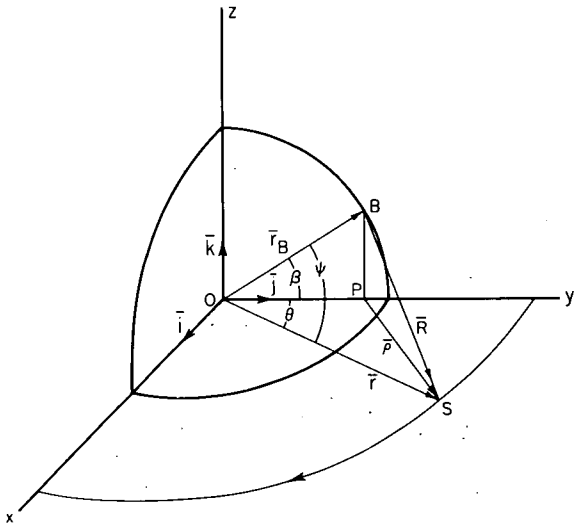

Figure 5.- Circular orbit geometry.

Consider the coordinate system of figure 5. The coordinate axes are alined with the xy plane in the orbit plane of the satellite and with the beacon located at a point B above the y axis (x = 0) on the lunar surface. The moon is assumed not to rotate with respect to the coordinate system. The beacon is located by the vector

$$\bar{r}_B = r_B \cos\beta\bar{j} + r_B \sin\beta\bar{k} \tag{45}$$

The satellite is located by the vector

$$\bar{r} = (r \sin\dot{\theta}t)\bar{i} + (r \cos\dot{\theta}t)\bar{j} \tag{46}$$

Note that when t = 0 the satellite is at the point of nearest approach to the beacon. The angle ψ between $\bar{r}_B$ and $\bar{r}$ is found using the definition of the dot product, with the result that

$$\cos\psi = \cos\beta \cos\dot{\theta}t \tag{47}$$

Application of the law of cosines to triangle $\overline{OBS}$ and of equation (47) results in

$$R^2 = r_B{}^2 + r^2 - 2r_B r \cos\beta \cos\dot{\theta}t \tag{48}$$

The law of cosines applied to triangle $\overline{OPS}$ yields

$$\rho^2 = r^2 + (r_B \cos\beta)^2 - 2rr_B \cos\beta \cos\dot{\theta}t \tag{49}$$

Equation (49) is differentiated with respect to time to give

$$\rho\dot{\rho} = \dot{\theta}rr_B \cos\beta \sin\dot{\theta}t \tag{50}$$

A relationship between ρ and R can be obtained by use of the Pythagorean theorem on right triangle $\overline{PBS}$

$$R^2 = (r_B \sin\beta)^2 + \rho^2 \tag{51}$$

Equation (51) is differentiated with respect to time and solved for $\dot{R}$.

$$\dot{R} = \frac{\rho\dot{\rho}}{R} \tag{52}$$

Then equation (50) is substituted into (52) to give $\bar{R}$ as a function of range and time.

$$\dot{R} = \frac{\dot{\theta} r r_B \cos\beta \sin\dot{\theta}t}{R} \tag{53}$$

Range can be eliminated from (53) with the aid of equation (48).

$$\dot{R} = \frac{\dot{\theta} r r_B \cos\beta \sin\dot{\theta}t}{\sqrt{r_B^2 + r^2 - 2rr_B \cos\beta \cos\dot{\theta}t}} \tag{54}$$

Equation (54) expresses the instantaneous range rate of the satellite with respect to the beacon as a function of time. The average range rate over a time interval T is found by integrating equation (54).

$$\dot{R}_a = \frac{1}{T}\int_{t-\frac{T}{2}}^{t+\frac{T}{2}} \dot{R}\,dt = \frac{1}{T}\int_{t-\frac{T}{2}}^{t+\frac{T}{2}} \frac{\dot{\theta} r r_B \cos\beta \sin\dot{\theta}t}{\sqrt{r_B^2 + r^2 - 2rr_B \cos\beta \cos\dot{\theta}t}}\,dt \tag{55}$$

With the change of variable $u = \cos\dot{\theta}t$, equation (54) can be integrated.[5] The result is

$$\dot{R}_a = \frac{\sqrt{2rr_B \cos\beta}}{T}\left\{\left[\frac{r_B^2 + r^2}{2rr_B \cos\beta} - \cos\dot{\theta}\left(t + \frac{T}{2}\right)\right]^{1/2} - \left[\frac{r_B^2 + r^2}{2rr_B \cos\beta} - \cos\dot{\theta}\left(t - \frac{T}{2}\right)\right]^{1/2}\right\} \tag{56}$$

Equation (56) can be simplified by trigonometric identities so that

$$\dot{R}_a = \frac{\sqrt{2rr_B \cos\beta}}{T}\left[\left(\frac{r_B^2 + r^2}{2rr_B \cos\beta} - \cos\frac{\dot{\theta}T}{2}\cos\dot{\theta}t + \sin\frac{\dot{\theta}T}{2}\sin\dot{\theta}t\right)^{1/2} - \left(\frac{r_B^2 + r^2}{2rr_B \cos\beta} - \cos\frac{\dot{\theta}T}{2}\cos\dot{\theta}t - \sin\frac{\dot{\theta}T}{2}\sin\dot{\theta}t\right)^{1/2}\right] \tag{57}$$

---

[5] Integral 191.01, page 46, reference 16.

Time can be eliminated from equation (57) by solving equation (48) for $\cos \dot{\theta}t$,

$$\cos \dot{\theta}t = \frac{r_B^2 + r^2 - R^2}{2rr_B \cos \beta} \tag{58}$$

and equation (53) for $\sin \dot{\theta}t$,

$$\sin \dot{\theta}t = \frac{R\dot{R}}{\dot{\theta}rr_B \cos \beta} \tag{59}$$

and substituting (58) and (59) into (57):

$$\dot{R}_a = \frac{\sqrt{2rr_B \cos \beta}}{T}\left[\left(\frac{r_B^2 + r^2}{2rr_B \cos \beta} - \frac{r_B^2 + r^2 - R^2}{2rr_B \cos \beta} \cos \frac{\dot{\theta}T}{2} - \frac{R\dot{R}}{\dot{\theta}rr_B \cos \beta} \sin \frac{\dot{\theta}T}{2}\right)^{1/2}\right.$$

$$\left. - \left(\frac{r_B^2 + r^2}{2rr_B \cos \beta} - \frac{r_B^2 + r^2 - R^2}{2rr_B \cos \beta} \cos \frac{\dot{\theta}T}{2} - \frac{R\dot{R}}{\dot{\theta}rr_B \cos \beta} \sin \frac{\dot{\theta}T}{2}\right)^{1/2}\right] \tag{60}$$

For a typical lunar orbit the angular velocity $\dot{\theta}$ is of the order of 10^{-3} rad/sec. Therefore, $\dot{\theta}T/2 \ll 1$ and equation (60) can be simplified by letting $\sin \dot{\theta}T/2 = \dot{\theta}T/2$ and $\cos \dot{\theta}T/2 = 1$. The result is

$$\dot{R}_a = \frac{1}{T}(R^2 + TR\dot{R})^{1/2} - \frac{1}{T}(R^2 - TR\dot{R})^{1/2} \tag{61}$$

The averaging time error for a circular orbit, using equation (44), is equal to

$$\Delta\dot{R} = \dot{R} - \frac{1}{T}(R^2 + TR\dot{R})^{1/2} + \frac{1}{T}(R^2 - TR\dot{R})^{1/2} \tag{62}$$

For the special case where $\dot{R} < R/T$ (this is generally true for most cases of practical interest) the quantities $(R^2 \pm TR\dot{R})^{1/2}$ in equation (62) can each be expanded by the binomial theorem.

$$(R^2 \pm TR\dot{R})^{1/2} = R \pm \frac{1}{2}\dot{R}T - \frac{1}{8}\frac{\dot{R}^2T^2}{R} \pm \frac{1}{16}\frac{\dot{R}^3T^3}{R^2} - \frac{5}{128}\frac{\dot{R}^4T^4}{R^3} \pm \frac{7}{256}\frac{\dot{R}^5T^5}{R^4} - \cdots \tag{63}$$

Substitution of (63) into (62) yields

$$\Delta\dot{R} = -\frac{T^2\dot{R}^3}{8R^2} - \frac{7T^4\dot{R}^5}{128R^4} - \cdots \tag{64}$$

If $\dot{R}$ is sufficiently less than R/T so that the second term of (64) is negligible, the range-rate error due to the averaging time error in a circular orbit becomes

$$\Delta\dot{R} = -\frac{T^2\dot{R}^3}{8R^2} \tag{65}$$

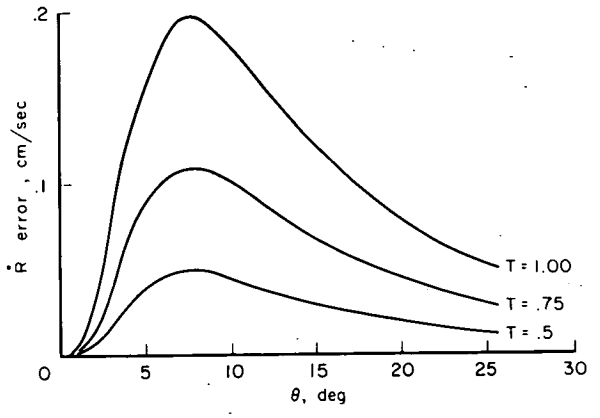

Figure 6.- Range rate averaging time error for satellite in circular lunar orbit; altitude = 200 km, $\beta = 0^\circ$.

In figure 6 the averaging time error is plotted against the angular displacement θ of the satellite in its orbit ($\theta = 0$ corresponds to the point of closest approach to the beacon) for various values of Doppler averaging time, T.

Finite propagation time error.- The Doppler-shifted frequency transponded by the beacon to the satellite is related to a range rate $\dot{R}(t)$. This signal arrives at the satellite at time $t + \tau/2$, where $\tau/2$ is the one-way propagation time, and is detected to yield $\dot{R}(t)$. However, the true range rate at the instant of reception is $\dot{R}(t + \tau/2)$. Therefore, there is an error in the range-rate measurement equal to

$$\Delta\dot{R} = \dot{R}\left(t + \frac{\tau}{2}\right) - \dot{R}(t) \tag{66}$$

$$\Delta\dot{R} = \dot{R}(t) + \int_t^{t+\frac{\tau}{2}} \ddot{R}\, dt - \dot{R}(t) \tag{67}$$

$$\Delta\dot{R} = \int_t^{t+\frac{\tau}{2}} \ddot{R}\, dt \tag{68}$$

In the case of a lunar satellite typical propagation times will be very small, usually no more than 10^{-2} second. Therefore, equation (68) can be simplified to

$$\Delta\dot{R} = \frac{\ddot{R}\tau}{2} = \ddot{R}\left(\frac{R}{c}\right) \tag{69}$$

For a circular orbit equation (53) can be rearranged to give

$$R\dot{R} = \dot{\theta}rr_B \cos\beta \sin\dot{\theta}t \tag{70}$$

and differentiated with respect to time to give

$$\ddot{R}R = \dot{\theta}^2 r r_B \cos\beta \cos\dot{\theta}T - \dot{R}^2 \tag{71}$$

Substituting equation (71) into (69) and eliminating $\cos\dot{\theta}t$ with equation (58) gives the finite propagation time error for a circular orbit.

$$\Delta\dot{R} = \frac{\dot{\theta}^2}{2c}\left(r_B^2 + r^2 - R^2\right) - \frac{1}{c}\dot{R}^2 \tag{72}$$

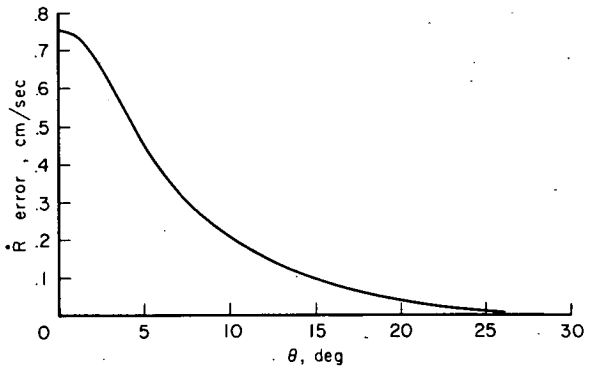

Figure 7.- Range rate finite propagation time error for satellite in circular lunar orbit; altitude = 200 km, $\beta = 0^\circ$.

Figure 7 shows the finite propagation time error in range rate versus the angular displacement of the satellite for a circular orbit. It is seen that this error is a minimum when R (and hence the propagation time) is a maximum and increases to a maximum at $\theta = 0$ when R is a minimum. This is because as θ decreases, the range acceleration $\ddot{R}$ increases faster than the range R decreases, so that the product $\ddot{R}R$ in equation (69) increases as θ decreases. In this sense the $\ddot{R}$ term of equation (69) dominates this error.

RANGE

The Ranging Principle

If the interrogator carrier signal is phase modulated with a low-frequency sinusoidal tone, it is possible to measure range. This is possible because the signal transmitted by the interrogator requires a finite time τ to complete the trip to the beacon and back to the interrogator. Therefore, there will be a phase difference φ_m between the transmitted signal and the received signal equal to

$$\varphi_m = \omega_m \tau \tag{73}$$

The two-way propagation time τ is approximated by $\tau = 2R/c$ so that equation (73) becomes

$$\varphi_m = \frac{4\pi f_m R}{c} \tag{74}$$

Equation (74) can be solved for the range to give the range equation

$$R = \frac{c\,\varphi_m}{4\pi f_m} \tag{75}$$

The maximum unambiguous phase angle φ_m is 2π radians, which results in a maximum unambiguous range of

$$R_{max} = \frac{c(2\pi)}{4\pi f_m} = \frac{c}{2f_m} = \frac{\lambda_m}{2} \tag{76}$$

Therefore, the wavelength of the ranging tone should be equal to or greater than twice the maximum expected range if there is no way of resolving the range ambiguity. For example, an 800 Hz ranging tone has a maximum unambiguous range of 187.3 km.

However, the phase angle φ_m cannot be measured exactly. For the particular system described in reference 1 the overall phase measurement accuracy is about one percent of full range or 3.6° in phase. This means that the range resolution of the 800 Hz tone would be 1.873 km. To improve the resolution, the carrier is phase modulated with additional higher frequency ranging tones. The low-frequency tones are used only to remove the range ambiguity of the high-frequency tones. For example, a 100 kHz high-frequency ranging tone would have a resolution of 15 m.

Description of the Ranging System

The basic block diagram of the interrogator portion of the ranging system is shown in figure 8. The portion within the dashed line is the same equipment as that enclosed within the dashed line of the range rate system in figure 1.

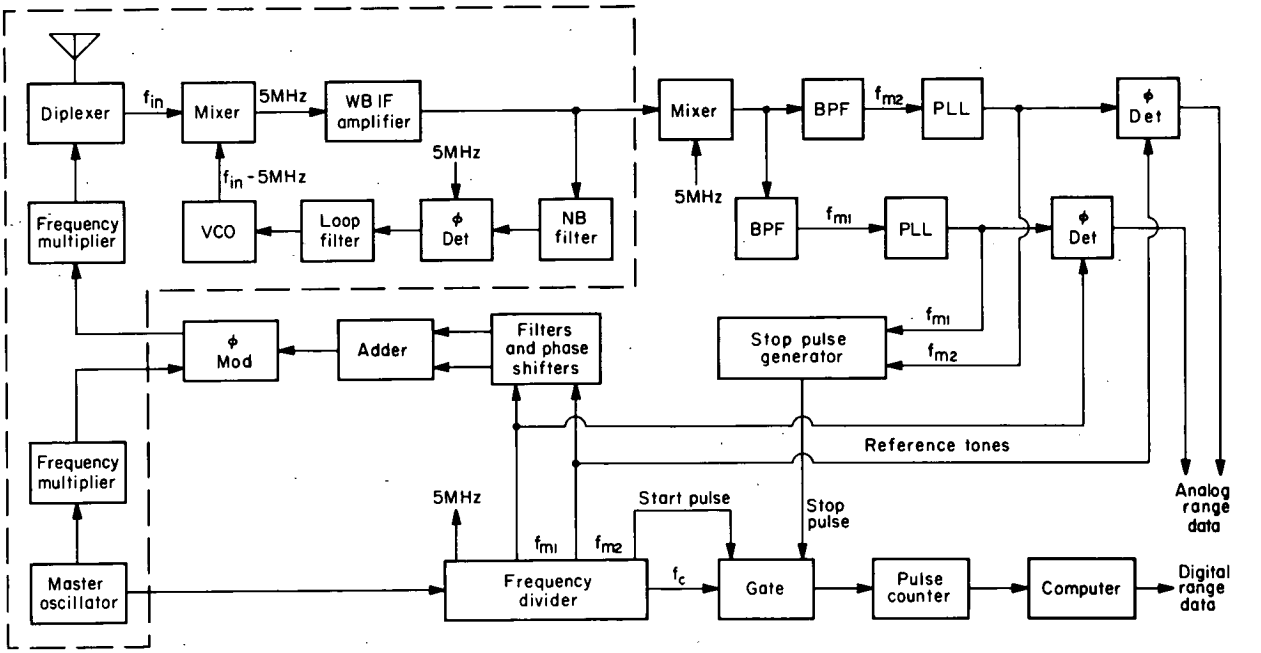

Figure 8.- Ranging system.

The ranging tones are generated by frequency division of a stable master oscillator frequency. The output of the frequency dividers is several coherent square wave ranging tones (two, f_{m_1} and f_{m_2}, are shown in fig. 8) which are filtered to provide sine waves and fed to individual phase shifters which adjust the phase of each tone and remove any differential phase shift that may be present in the system. The properly phased coherent ranging tones then phase modulate the carrier and are transmitted to the transponder. The transponder receives the signal, amplifies it, and retransmits it back to the interrogator. The beacon transponder equipment is the same as that used in the range-rate measuring system.

The receiver PLL within the dashed portion serves a dual role as a narrowband tracking filter and as the first IF stage. Therefore, the PLL output is a carrier at a constant IF frequency and phase modulated with the ranging tones. These are passed through a bandpass filter bank to separate the individual ranging tones, and each tone is then tracked with a second PLL to further improve the signal-to-noise ratio. It should be noted that each ranging tone has a slight Doppler shift. This Doppler shift could be removed by a phase-locked loop, but it is a deterministic error and so can more easily be removed by a computer during data reduction. This error is analyzed in a later section.

The phase angles of the ranging tones are measured in either of two ways: (1) by comparison with a reference (transmitted) tone in a phase detector, or (2) by means of an all digital pulse counting technique. In the first case, the phase detector output is an analog voltage proportional to the phase difference between the transmitted and received signals. In the second case, the received ranging tones, by means of a stop-pulse generator, determine the length of time that a counter gate is open. This time interval determines the number of pulses of frequency f_c which are counted by the pulse counter, and this count is proportional to the range. A detailed description of the operation of the stop-pulse generator is given in references 1 and 2.

Stochastic Errors

Master oscillator short-term instability.- The ranging system works on the principle of measuring the phase difference between the transmitted and received ranging tones. Clearly then, the ranging frequencies must have good phase, and hence frequency, stability, if an accurate phase comparison is to be made.

Consider the transmitted and received ranging tones at the input of the phase detector. The reference (transmitted) ranging tone can be represented as

$$y_t(t) = \sin[\omega_m t + \varphi(t)] \tag{77}$$

where ω_m is the ranging tone radian frequency and $\varphi(t)$ is the phase noise of the oscillator output. The received tone is

$$y_r(t) = \sin[\omega_m(t - \tau) + \varphi(t - \tau)] \tag{78}$$

The output of the phase detector is proportional to the phase difference

$$\varphi_m(t) = \omega_m\tau + \varphi(t) - \varphi(t - \tau) \tag{79}$$

The range, from equation (75), is

$$R = \frac{c\tau}{2} + \frac{c}{2\omega_m}[\varphi(t) - \varphi(t - \tau)] \tag{80}$$

The rms error in the range measurement due to oscillator instability is therefore equal to

$$\sigma_R = \frac{c}{2\omega_m}\left[\overline{\varphi(t)^2} - \overline{2\varphi(t)\varphi(t - \tau)} + \overline{\varphi(t - \tau)^2}\right]^{1/2} \tag{81}$$

where the bar means "average." The technique used in the discussion of range rate short-term oscillator instability can be used to write equation (81) in terms of the autocorrelation function of the phase noise $\varphi(t)$ as

$$\sigma_R = \frac{c}{\sqrt{2}\omega_m}[R(0) - R(\tau)]^{1/2} \tag{82}$$

Over the narrow bandwidth of the ranging tone receiver the phase fluctuation $\varphi(t)$ is approximately white noise. Therefore, assume it has a two-sided power spectral density of low pass filtered white noise

$$G_\varphi(\omega) = \frac{2\sigma_p{}^2\nu}{\omega^2 + \nu^2} \tag{83}$$

The autocorrelation function $R(\tau)$ can be found by the inverse Fourier transform of $G_\varphi(\omega)$

$$R(\tau) = \frac{1}{2\pi}\int_{-\infty}^{\infty} G_\varphi(\omega)e^{j\omega\tau}\,d\omega \tag{84}$$

Because of even symmetry

$$R(\tau) = \frac{2\sigma_p{}^2\nu}{\pi}\int_0^{\infty} \frac{\cos\tau}{\omega^2 + \nu^2} \tag{85}$$

Equation (85) can be integrated with tables[6] to yield

$$\Re(\tau) = \sigma_p^2 e^{-\nu|\tau|} \tag{86}$$

A physical interpretation of ν can be found by considering the noise equivalent bandwidth (ref. 17), B:

$$B = \frac{\text{Total power}}{\text{Peak power}} = \frac{\int_{-\infty}^{\infty} G_\varphi(\omega)d\omega}{G_\varphi(0)} \tag{87}$$

The noise equivalent bandwidth is the bandwidth of a rectangular power spectral density with height $G_\varphi(0)$ and with an area equal to that under $G_\varphi(\omega)$. Substituting equation (83) into (87) yields

$$B = \frac{2\sigma^2\pi}{2\sigma^2/\nu} = \nu\pi \frac{\text{rad}}{\text{sec}} = \frac{\nu}{2} \text{ Hz} \tag{88}$$

Thus, ν is equal to twice the noise equivalent bandwidth of the phase fluctuation.

The physical interpretation of σ_p^2 is easily seen by noting that $\Re(0) = \sigma_p^2 =$ mean square power. Since the phase fluctuation has zero mean, σ_p^2 is the variance of the phase fluctuation.

Equation (86) is substituted into (82) to obtain the rms range error due to short-term oscillator instability.

$$\sigma_R = \frac{c}{\sqrt{2}\omega_m}\left(\sigma_p^2 - \sigma_p^2 e^{-\nu|\tau|}\right)^{1/2} \tag{89}$$

Most oscillator phase noise is approximately white noise; therefore, ν is large. In this case equation (89) can be simplified to

$$\sigma_R = \frac{c\sigma_p}{\sqrt{2}\omega_m} \tag{90}$$

If the oscillator rms fractional frequency instability is $S_s = \Delta f_m/f_m$, then the rms phase deviation σ_p is

$$\sigma_p = 2\pi\left(\frac{\Delta f_m}{f_m}\right) f_m\tau \tag{91}$$

---

[6]Integral 859.001, page 224, reference 16.

Substituting equation (91) into (90) and letting $\tau = 2R/c$ yields

$$\sigma_R = \sqrt{2}\, S_s R \tag{92}$$

This is a noise-type error.

Master oscillator long-term instability.- The error in range due to the master oscillator long-term instability is a bias-type error caused by an uncertainty in the modulating frequency f_m. The error is calculated by differentiating equation (75) with respect to f_m and substituting the derivative into the total differential,

$$\Delta R = \frac{\partial R}{\partial f_m} \Delta f_m = \left(\frac{c\varphi}{4\pi f_m}\right)\left(\frac{\Delta f_m}{f_m}\right) \tag{93}$$

Since the first term in parentheses is the range R and the second term is the long-term rms fractional frequency stability factor S_L, equation (93) becomes

$$\sigma_R = S_L R \tag{94}$$

Quantization error.- In the digital range measuring scheme the master oscillator generates a start pulse which opens an electronic gate and allows a pulse counter to count pulses of frequency f_c. At a later time, equal to the two-way propagation time τ, the coherent ranging tones generate a stop pulse which closes the gate and stops the counter. The counter counts zero crossings of the pulses which pass through the gate; therefore, the counter has a resolution of only half a cycle. Since the stop pulse will generally not occur exactly at a zero crossing, the counter reading will always be a fraction of a half-cycle less than the true count (i.e., the counter counts to the nearest integer less than the true count).

In the time τ the counter (initially cleared) will count to

$$N = \tau f_c = \frac{2R}{c} f_c \tag{95}$$

The error in range due to a counting error ΔN is found by solving equation (95) for range, differentiating with respect to N and substituting the derivative into the total differential:

$$\Delta R = \frac{\partial R}{\partial N} \Delta N = \frac{c}{2f_c} \Delta N \tag{96}$$

There is a maximum count error ΔN_{max} of one count (negative) at the end of the count period. Therefore, the maximum range error, from equation (96), is $\Delta R_{max} = -c/2f_c$. There is no count error at the beginning of the count period because the start pulse is coherent with the transmitted ranging tones.

The method of analysis is analogous to the range-rate quantization error analysis. Thus, the mean range quantization error can be shown to be $\Delta R_{max}/2$ and the standard deviation to be $\Delta R_{max}/2\sqrt{3}$. Therefore, the mean range quantization error is

$$\text{mean } (\Delta R) = \frac{-c}{4f_c} \tag{97}$$

and the standard deviation of the range quantization error is

$$\sigma_R = \frac{c}{4\sqrt{3}\, f_c} \tag{98}$$

To obtain zero mean errors in range measurement, the mean error (eq. (97)) should be added to the range measurement. This could be done in the computer by adding half a count to N in equation (95) before computing the measured range.

Phase-locked loop error.- Since the ranging principle depends directly on the measurement of a phase angle difference, imperfect phase tracking of the ranging tone signal by the ranging tone PLL will cause an error in the range measurement. This section considers this error. The additive noise at the input of the PLL is assumed to be Gaussian and white. The PLL is assumed to be a second-order active loop similar to that discussed in the range-rate section.

The reference (transmitted) signal tone can be represented as

$$E_t(t) = \sin \omega_m t \tag{99}$$

and the received signal at the same instant is

$$E_r(t) = \sin \omega_m(t - \tau) + N(t) \tag{100}$$

where N(t) represents the additive Gaussian white noise. Jaffe and Rechtin (ref. 18) have shown that when the PLL is linearized, the additive noise can be represented as a phase noise $\varphi(t)$ if the phase error is small. Therefore, the received signal can be represented as

$$E_r(t) = \sin[\omega_m(t - \tau) + \varphi(t)] \tag{101}$$

The reference and received signals are phase detected to yield a signal proportional to the phase difference

$$\varphi_m(t) = \omega_m\tau - \varphi(t) \tag{102}$$

Substituting equation (102) into equation (75) yields

$$R = \frac{c\tau}{2} - \frac{c\varphi(t)}{2\omega_m} \tag{103}$$

The second term of equation (103) represents the error in the range measurement. The rms range error is

$$\sigma_R = \frac{c}{2\omega_m}\sqrt{\overline{\varphi^2(t)}} = \frac{c}{2\omega_m}\sqrt{\Re(0)} \tag{104}$$

where the bar means "average," and $\Re(0)$ is the autocorrelation function $\Re(t)$ with the correlation time equal to zero. But $\Re(0)$ in equation (104) is identical in form to $\Re(0)$ in equation (32). Therefore, the rms range error due to additive phase noise is

$$\sigma_R = \frac{c}{4\omega_m}\left(\frac{\Phi_R\omega_n}{2}\,\frac{1 + 4\zeta^2}{\zeta}\right)^{1/2} \tag{105}$$

If N_R is the power spectral density of the phase noise $\varphi(t)$, then letting $\Phi_R = K_R R^2$, as in the case of the range-rate PLL error equation (36), equation (105) becomes

$$\sigma_R = \frac{cR}{8\pi f_m}\left(\frac{K_R\omega_n}{2}\,\frac{1 + 4\zeta^2}{\zeta}\right)^{1/2} \tag{106}$$

Phase detector error.- A phase detector does not measure a phase difference without error. Therefore, if the range is determined by measuring the phase difference between the received and transmitted ranging tones, the phase detector error must be considered.

The error in range produced by the inaccuracy of the phase detector is found by differentiating equation (75) with respect to φ_m and substituting the derivative into the total differential.

$$\Delta R = \frac{\pi}{180}\,\frac{\partial R}{\partial \varphi_m}\,\Delta\varphi_m \tag{107}$$

where $\Delta\varphi_m$ is the amount of phase error introduced by the phase detector expressed in degrees. If σ_{PD} is the rms value of $\Delta\varphi_m$, the rms range error due to the phase detector error is

$$\sigma_R = \frac{c\sigma_{PD}}{720f_m} \tag{108}$$

This error exists in a ranging system only if range is measured by the phase detector method. If range is measured with the digital pulse-counting method, the system will have quantization error instead.

Calibration drift error.- The ranging system requires the correct phase relationship between the ranging tones. Adjustable phase shifters are, therefore, incorporated in the circuitry to insure the proper phase relationships and to remove the phase bias errors inherent in the transmitting and receiving equipment. A range measurement error results whenever the phase shift calibration drifts.

Calibration drift is a significant source of error with ranging equipment subjected to environmental extremes. Such errors vary widely with equipment and environment, and usually can be determined only experimentally. A representative 3σ value for the overall system calibration error (ref. 3) is 0.869°. Thus, the standard deviation in phase drift σ_{CD} is 0.289°. The standard deviation in range is found by substituting the rms phase drift σ_{CD} into equation (107). The result is

$$\sigma_R = \frac{c\sigma_{CD}}{720f_m} \tag{109}$$

This is a bias-type error (provided that the phase drift does not change significantly during the time period of interest).

Uncertainty in the speed of light.- It can be seen from equation (75) that the conversion of measured phase angle φ_m to range requires a knowledge of the velocity of light. However, since there is an uncertainty in the exact value of c, there is a range error equal to

$$\Delta R = \frac{\partial R}{\partial c}\Delta c = \frac{c\varphi_m}{4\pi f_m}\frac{\Delta c}{c} = R\frac{\Delta c}{c} \tag{110}$$

where $\partial R/\partial c$ is found by differentiating equation (75). The 1σ uncertainty is 3.33×10^{-7}, so that the rms range error due to the uncertainty in the speed of light is

$$\sigma_R = (3.33\times10^{-7})R \tag{111}$$

This is a bias-type error.

Deterministic Errors

Finite propagation time error.- There exists a finite propagation time error in the range measurement analogous to that described for the range rate. (For the following analysis refer to figure 5.)

Equation (48) gives the beacon-to-satellite range at the instant the beacon transponds. The satellite measures this value which will be called R_m.

$$R_m = \sqrt{r_B^2 + r^2 - 2rr_B \cos \beta \cos \dot{\theta}t} \tag{112}$$

A better estimate of the range is

$$\hat{R} = \sqrt{r_B^2 + r^2 - 2rr_B \cos \beta \cos \dot{\theta}(t + R_m/c)} \tag{113}$$

where $t + R_m/c$ is the time at which the ranging tones are received. Normally $\dot{\theta}R_m/c \ll 1$ so that equation (113) simplifies to

$$\hat{R} = \sqrt{r_B^2 + r^2 - 2rr_B \left(\cos \dot{\theta}t - \frac{\dot{\theta}R_m}{c} \sin \dot{\theta}t\right) \cos \beta} \tag{114}$$

Equation (112) can be substituted into (114) to give

$$\hat{R} = \sqrt{R_m^2 + \frac{2rr_B\dot{\theta} \cos \beta}{c} R_m \sin \dot{\theta}t} \tag{115}$$

The finite propagation time error is equal to

$$\Delta R = \hat{R} - R_m \tag{116}$$

Therefore,

$$\Delta R = \sqrt{R_m^2 + \frac{2rr_B\dot{\theta} \cos \beta}{c} R_m \sin \dot{\theta}t} - R_m \tag{117}$$

The explicit dependence of ΔR on time is removed by substituting equation (59) into (117) with the result that

$$\Delta R = R_m\left(\sqrt{1 + \frac{2\dot{R}}{c}} - 1\right) \tag{118}$$

Since $2\dot{R}/c \ll 1$ for typical orbits, the square root term of equation (118) can be expanded with the binomial expansion

$$\sqrt{1 + \frac{2\dot{R}}{c}} \approx 1 + \frac{\dot{R}}{c} \tag{119}$$

Therefore,

$$\Delta R = \frac{R\dot{R}}{c} \tag{120}$$

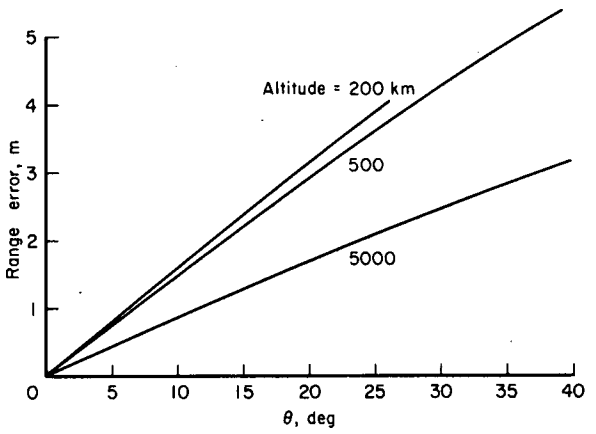

Figure 9.- Range finite propagation time error for satellite in circular lunar orbit; $\beta = 0^{\circ}$.

Figure 9 shows the finite propagation time error in range versus the angular displacement θ of the satellite for various circular orbit altitutdes. The curves terminate at values of θ at which the satellite recedes below the lunar horizon.

Doppler shift of the ranging tones.- If τ is the two-way propagation time, the phase angle of a ranging tone with no Doppler shift is

$$\varphi_m = 2\pi f_m \tau \tag{121}$$

For the Doppler shifted signal the phase angle is

$$\varphi_{md} = 2\pi(f_m + f_{md})\tau \tag{122}$$

The error in the phase angle measurement is

$$\Delta\varphi_m = \varphi_{md} - \varphi_m = 2\pi f_{md}\tau \tag{123}$$

Substituting equation (123) into (75) and letting $\tau = 2R/c$ gives

$$\Delta R = \left(\frac{f_{md}}{f_m}\right) R \tag{124}$$

But from appendix A

$$f_m + f_{md} = \frac{c + \dot{R}}{c - \dot{R}} f_m \tag{125}$$

which can be solved for f_{md}/f_m to give

$$\frac{f_{md}}{f_m} = \frac{2R}{c - \dot{R}} \tag{126}$$

Therefore, the error in range due to a Doppler shift in the ranging tone is equal to

$$\Delta R = \frac{2R}{c - \dot{R}} f_m \tag{127}$$

TOTAL ERROR MODEL NUMERICAL EXAMPLES

This section gives expressions for the root-sum-square (rss) range and range-rate stochastic errors for typical system parameters. The deterministic errors are not included because they can be removed during data reduction. If the individual stochastic errors described in the previous sections are considered to be (1σ) standard deviations of independent random processes, then the overall range and range-rate variances can be found by summing the individual variances.

The following typical parameters are used for the numerical example:

f_c	10MHz
f_m	100kHz
f_o	200kHz
f_t	1.7GHz
G_r	1
G_t	1
K	1
N_R	2.5×10^{-21} W/Hz
N_V	4×10^{-20} W/Hz
P_t	1 W
S_L	1×10^{-6}
S_s	1×10^{-9}
T	1 sec
ζ	0.5
σ_{CD}	0.289°
σ_{PD}	1°
ω_n	6.28 rad/sec

Assume that the satellite is in a circular orbit about the moon with an altitude of 200 km, and the beacon latitude is 0^{o} (overhead pass).

The rss range-rate error is:

$$\sigma_{\dot{R}} = \Bigg\{ \begin{cases} (3\times10^{-10})R & \text{for } 0 \le R \le 1.5\times10^{8} \\ 4.5\times10^{-2} & \text{for } R \ge 1.5\times10^{8} \end{cases}$$

Master oscillator short-term frequency instability (eq. (16))

$$+ (1\times10^{-12})\dot{R}^2$$

Master oscillator long-term frequency instability (eq. (19))

$$+ 3.24\times10^{-4}$$

Quantization (eq. (25))

$$+ (24.4\times10^{-20})R^2$$

Phase-locked loop (eq. (37))

$$+ (\dot{R} + 1.77\times10^{4})^2\, 10^{-18}$$

Uncertainty in Doppler averaging time (eq. (41))

$$+ (1.11\times10^{-13})\dot{R}^2 \Bigg\}^{1/2} \text{ m/sec}$$

Uncertainty in speed of light (eq. (43))

(128)

where R is in meters and $\dot{R}$ is in m/sec. It is seen that the largest error in range rate is caused by the master oscillator short-term frequency instability and by the quantization process.

The rss range error is

$$\sigma_{R} = \Big\{ (2\times10^{-18})R^2$$

Master oscillator short-term frequency instability (eq. (92))

$$+ (1\times10^{-12})R^2$$

Master oscillator long-term frequency instability (eq. (94))

$$+ (2.28\times10^{-12})R^2$$

Phase-locked loop (eq. (106))

$$+ \begin{matrix} 18.7 \text{ (quantization)} \\ 17.4 \text{ (phase detector)} \end{matrix}$$

(eq. (98))
(eq. (108))

$$+ 1.45$$

Calibration drift (eq. (109))

$$+ (1.11\times10^{-13})R^2 \Big\}^{1/2} \text{ meters}$$

Uncertainty in speed of light (eq. (111))

(129)

It is seen that the range error due to oscillator short-term frequency instability is negligible compared to the other error sources.

Equations (128) and (129) are plotted against angular displacement θ in figures 10 and 11. For the example orbits the range R is always less than 1.5×10^8 m, so that the first term of (128) is dependent on R.

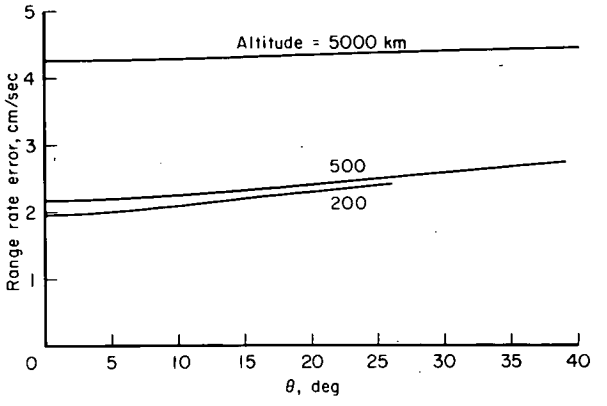

Figure 10.- Total range rate error for satellite in circular lunar orbit; $\beta = 0^\circ$, T = 1 sec.

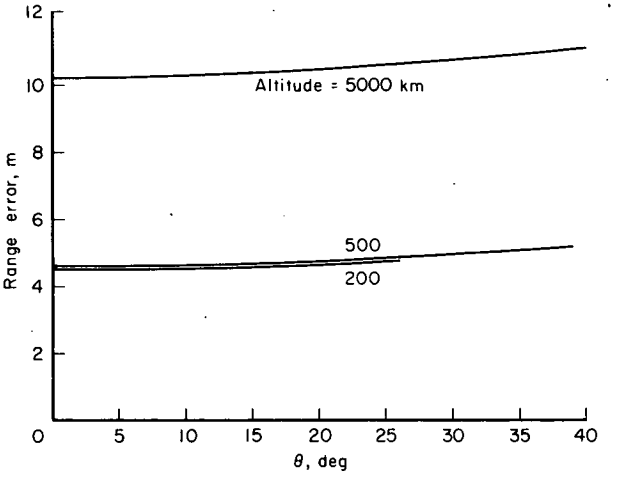

Figure 11.- Total range error for satellite in circular lunar orbit; $\beta = 0^\circ$.

CONCLUDING REMARKS

The descriptions of tracking system errors given constitute a reasonably complete error model for an interrogator-transponder type range and range-rate system. No attempt has been made here to evaluate the relative significance of the various types of errors since this depends upon the particular system and tracking mission considered. Generally, when the results are applied to a specific case, it will be found that only a few of the errors need to be included.

Ames Research Center
National Aeronautics and Space Administration
Moffett Field, Calif., 94035, Sept. 6, 1967
125-17-05-01-00-21

APPENDIX A

DERIVATION OF THE DOPPLER SHIFT EQUATION

The satellite approaches the beacon transponder and transmits with frequency f_t. The transponder receives this signal at frequency

$$f_{r_1} = \left(\frac{c + \dot{R}}{c - \dot{R}}\right)^{1/2} f_t \tag{A1}$$

in accordance with the standard equation describing the Doppler effect (ref. 19). The beacon retransmits with frequency

$$f_{t_2} = \left(\frac{c + \dot{R}}{c - \dot{R}}\right)^{1/2} f_t + f_L \tag{A2}$$

Finally, the satellite receives the transponded signal at frequency

$$f_{r_2} = \left[\left(\frac{c + \dot{R}}{c - \dot{R}}\right)^{1/2} f_t + f_L\right]\left(\frac{c + \dot{R}}{c - \dot{R}}\right)^{1/2} \tag{A3}$$

$$f_{r_2} = \left(\frac{c + \dot{R}}{c - \dot{R}}\right) f_t + \left(\frac{c + \dot{R}}{c - \dot{R}}\right)^{1/2} f_L \tag{A4}$$

By definition

$$f_t + 2f_{td} = \left(\frac{c + \dot{R}}{c - \dot{R}}\right) f_t \tag{A5}$$

and

$$f_L + f_{Ld} = \left(\frac{c + \dot{R}}{c - \dot{R}}\right)^{1/2} f_L \tag{A6}$$

Equation (A5) is solved for the range rate $\dot{R}$ giving

$$\dot{R} = \frac{cf_{td}}{f_{td} + f_t} \tag{A7}$$

However, since $f_t \gg f_{td}$ equation (A7) can be simplified to

$$\dot{R} \approx \frac{cf_{td}}{f_t} \tag{A8}$$

If the vehicle and beacon are moving away from each other, the result is exactly the same.

APPENDIX B

AVERAGING TIME AND FINITE PROPAGATION TIME ERRORS FOR ELLIPTIC AND HYPERBOLIC ORBITS

Figure 12 illustrates the orbit configuration to be considered. The rectangular coordinate system has its origin located at one focus of the conic

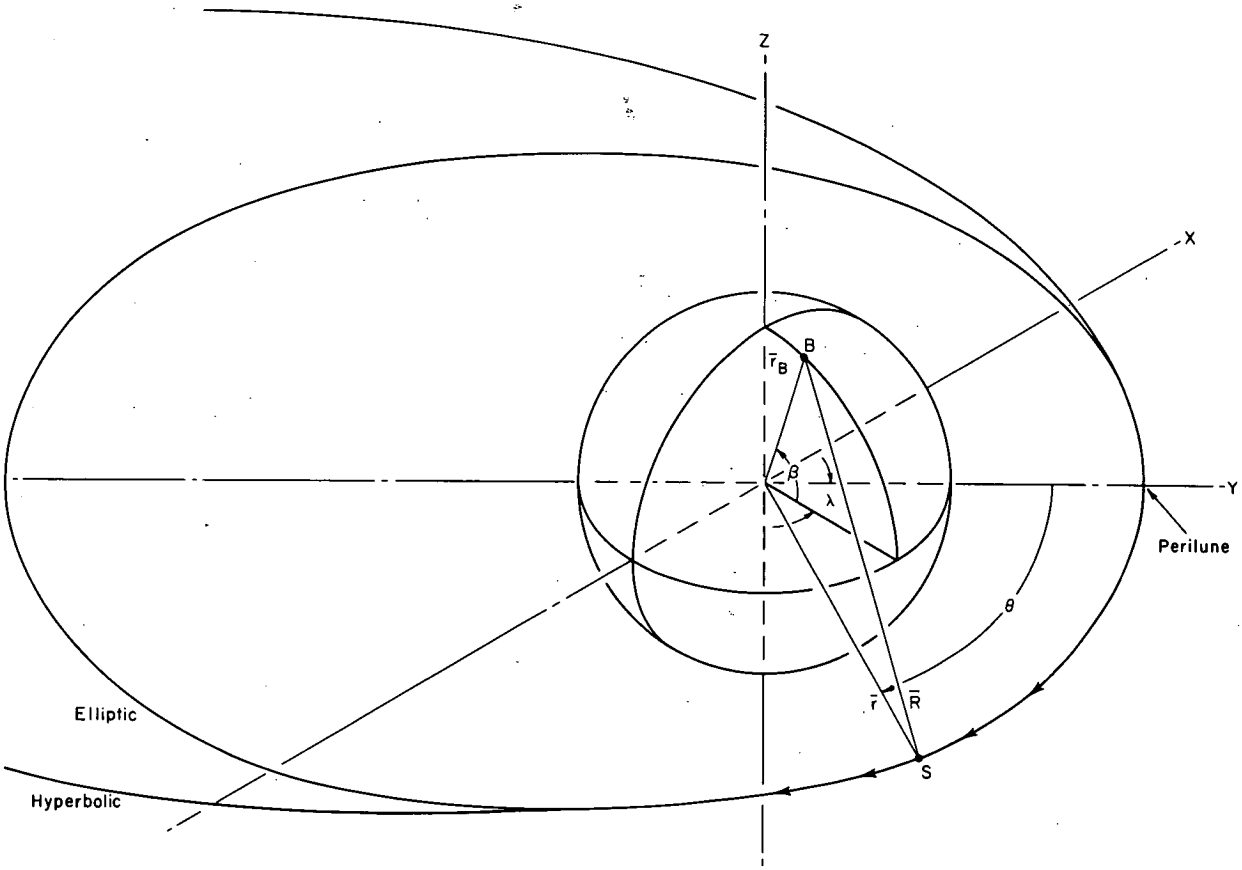

Figure 12.- Orbit configuration.

and is arranged with its xy plane in the satellite's orbital plane and with the y axis in the direction of the perilune. The beacon is located by longitude λ and latitude β. The satellite is located in the orbit by the true anomaly θ. The elliptic orbit will be considered first.

Three basic equations from the celestial mechanics of elliptic orbits that are useful in the subsequent analysis are given below without proof.[1]

[1]These are, respectively, equations 3-35, 3-36, and 3-40 of reference 20.

$$r \cos \theta = a(\cos E - e) \tag{B1}$$

$$r \sin \theta = a\sqrt{1 - e^2} \sin E \tag{B2}$$

$$nt = E - e \sin E \tag{B3}$$

where a is the semimajor axis of the satellite orbit, e is the eccentricity, E is the eccentric anomaly, and n is the mean angular velocity, $\sqrt{\mu/a^3}$.

Referring to figure 12 it is seen that:

$$\bar{r}_B = r_B \cos \beta \sin \lambda \bar{i} + r_B \cos \beta \cos \lambda \bar{j} + r_B \sin \beta \bar{k} \tag{B4}$$

$$\bar{r} = r \sin \theta \bar{i} + r \cos \theta \bar{j} \tag{B5}$$

and

$$\bar{R} = \bar{r} - \bar{r}_B \tag{B6}$$

Substituting equations (B4) and (B5) into (B6) yields

$$\bar{R} = (r \sin \theta - r_B \cos \beta \sin \lambda)\bar{i} + (r \cos \theta - r_B \cos \beta \cos \lambda)\bar{j} - r_B \sin \beta \bar{k} \tag{B7}$$

Equation (B7) is written in terms of the eccentric anomaly instead of the true anomaly by substituting equations (B1) and (B2) into (B7). The result is

$$\bar{R} = \left(a\sqrt{1 - e^2} \sin E - r_B \cos \beta \sin \lambda\right)\bar{i} + \left[a(\cos E - e) - r_B \cos \beta \cos \lambda\right]\bar{j} - r_B \sin \beta \bar{k} \tag{B8}$$

Equation (B8) is differentiated with respect to time to yield the range rate

$$\dot{\bar{R}} = a\sqrt{1 - e^2} \cos E \frac{dE}{dt} \bar{i} - a \sin E \frac{dE}{dt} \bar{j} \tag{B9}$$

assuming that the Moon does not rotate with respect to the coordinate system. The derivative dE/dt is obtained from equation (B3) and substituted into equation (B9) so that the range rate becomes

$$\bar{\dot{R}} = \frac{-an \sin E}{1 - e \cos E}\,\bar{i} + \frac{an\sqrt{1 - e^2}\cos E}{1 - e \cos E}\,\bar{j} \tag{B10}$$

The average range rate over an averaging time T is found by evaluating the integral

$$\bar{\dot{R}}_a = \frac{1}{T}\int_{t-\frac{T}{2}}^{t+\frac{T}{2}} \bar{\dot{R}}\, dt = \frac{\bar{i}}{T}\int_{t-\frac{T}{2}}^{t+\frac{T}{2}} \dot{X}\, dt + \frac{\bar{j}}{T}\int_{t-\frac{T}{2}}^{t+\frac{T}{2}} \dot{Y}\, dt \tag{B11}$$

Substituting the components of (B9) into (B11) and integrating yields

$$\bar{\dot{R}}_a = \frac{a\sqrt{1 - e^2}}{T}(\sin E_2 - \sin E_1)\bar{i} + \frac{a}{T}(\cos E_2 - \cos E_1)\bar{j} \tag{B12}$$

where E_1 is the eccentric anomaly corresponding to $t - (T/2)$; E_2 is the eccentric anomaly corresponding to $t + (T/2)$; and E_1 and E_2 are found by solving equation (B3). However, one cannot solve equation (B3) explicitly for E; therefore, some numerical scheme such as the Newton-Raphson method must be used.

An approximate method giving the average range rate $\bar{\dot{R}}_a$ as an explicit function of the true anomaly θ can be obtained by differentiating equation (B3) and substituting the derivative into the total differential

$$\Delta E = \frac{\partial E}{\partial t}\Delta t = \frac{n\,\Delta t}{1 - e \cos E} \tag{B13}$$

Then letting $\Delta t = T/2$, the approximate expressions for E_1 and E_2 are

$$E_1 = E - \frac{nT/2}{1 - e \cos E} \tag{B14}$$

$$E_2 = E + \frac{nT/2}{1 - e \cos E} \tag{B15}$$

Equations (B14) and (B15) are substituted into equation (B12) and the result is simplified by trigonometric identities to yield

$$\bar{\dot{R}}_a = \frac{2a\sqrt{1 - e^2}}{R}\sin\left(\frac{nT/2}{1 - e \cos E}\right)\cos E\bar{i} - \frac{2a}{T}\sin\left(\frac{nT/2}{1 - e \cos E}\right)\sin E\bar{j} \tag{B16}$$

Finally, equation (B16) is expressed in terms of the true anomaly θ by using the following equation[2] relating θ with the eccentric anomaly E:

$$E = 2 \arctan\left[\left(\frac{1 - e}{1 + e}\right)^{1/2} \tan\frac{\theta}{2}\right] \tag{B17}$$

Now the averaging time error can be calculated using the equation

$$\Delta\dot{R} = \dot{R} - \dot{R}_a \tag{B18}$$

In terms of the vector components of $\dot{\bar{R}}$ and $\dot{\bar{R}}_a$, equation (B18) can be written as

$$\Delta\dot{R} = \sqrt{\dot{X}^2 + \dot{Y}^2} - \sqrt{\dot{X}_a^2 + \dot{Y}_a^2} \tag{B19}$$

where $\dot{X}$, $\dot{Y}$, $\dot{X}_a$, $\dot{Y}_a$ are available from equations (B10) and (B16).

The range and range-rate finite propagation time errors are given approximately by equations (120) and (66), respectively. Evaluation of these equations requires that the magnitudes R, $\dot{R}$, and $\ddot{R}$ be known. The range magnitude R can be obtained from equation (B8), and the range-rate magnitude $\dot{R}$ can be obtained from equation (B10). An expression for the range acceleration $\ddot{R}$ can be obtained by differentiating equation (B10) with respect to time and eliminating dE/dt with the aid of equation (B3). The result is

$$\ddot{\bar{R}} = \frac{an^2\sqrt{1 - e^2}\sin E}{(1 - e\cos E)^3}\,\bar{i} - \frac{an^2(e - \cos E)}{(1 - e\cos E)^3}\,\bar{j} \tag{B20}$$

The analysis of a hyperbolic orbit is analogous to that of the elliptic orbit; therefore, only the results are stated here. The derivation of the results makes use of the following three equations from the celestial mechanics of hyperbolic orbits (note the similarity to eqs. (B1), (B2), and (B3)):

$$r\cos\theta = a(e - \cosh F) \tag{B21}$$

$$r\sin\theta = a\sqrt{e^2 - 1}\sinh F \tag{B22}$$

$$nt = e\sinh F - F \tag{B23}$$

where F is the eccentric anomaly in a hyperbolic orbit. The results are

[2]For derivation see page 51 of reference 20.

$$\bar{R} = (a\sqrt{e^2 - 1}\sinh F - r_B \cos\beta \sin\lambda)\bar{i}$$

$$+ [a(e - \cosh F) - r_B \cos\beta \cos\lambda]\bar{j} - r_B \sin\beta\bar{k} \tag{B24}$$

$$\dot{\bar{R}} = \frac{an\sqrt{e^2 - 1}\cosh F}{e\cosh F - 1}\bar{i} + \frac{-an\sinh F}{e\cosh F - 1}\bar{j} \tag{B25}$$

$$\ddot{\bar{R}} = \frac{-an\sqrt{e^2 - 1}\sinh F}{(e\cosh F - 1)^3}\bar{i} + \frac{an^2(\cosh F - e)}{(e\cosh F - 1)^3}\bar{j} \tag{B26}$$

$$\dot{\bar{R}}_a = \frac{a\sqrt{e^2 - 1}}{T}(\sinh F_2 - \sinh F_1)\bar{i} - \frac{a}{T}(\cosh F_2 - \cosh F_1)\bar{j} \tag{B27}$$

where F_1 is the eccentric anomaly corresponding to $t - \frac{T}{2}$; F_2 is the eccentric anomaly corresponding to $t + \frac{T}{2}$ and F_1 and F_2 are found by solving equation (B23) or by using the following approximate relationships:

$$F_1 = F - \frac{nT/2}{e\cosh F - 1} \tag{B28}$$

$$F_2 = F + \frac{nT/2}{e\cosh F - 1} \tag{B29}$$

These result in an approximate expression for the average range rate equal to:

$$\dot{\bar{R}}_a = \frac{2\sqrt{e^2 - 1}}{T}\sinh\left(\frac{nT/2}{e\cosh F - 1}\right)\cosh F\bar{i} + \frac{2a}{T}\sinh\left(\frac{nT/2}{e\cosh F - 1}\right)\sinh F\bar{j} \tag{B30}$$

Finally, the true anomaly θ is related to the eccentric anomaly F by the following equation:

$$F = 2 \operatorname{arc}\tanh\left[\left(\frac{e - 1}{e + 1}\right)^{1/2}\tan\frac{\theta}{2}\right] \tag{B31}$$

The averaging time error and range and range-rate finite propagation time errors are found using the above equations and equations (B19), (120), and (66).

REFERENCES

1. Habib, E. J.; Kronmiller, G. C., Jr.; Engels, P. D.; and Franks, H. J., Jr.: Development of a Range and Range Rate Spacecraft Tracking System. NASA TN D-2093, 1964.

2. Shaffer, H. W.; Kahn, W. D.; Bodin, W. J., Jr.; Kronmiller, G. C.; Engels, P. D.; and Habib, E. J.: The Range and Range Rate System and Data Analysis for Syncom I (1963 4A). NASA TN D-2139, 1964.

3. Anon.: AN/USQ-32 Microwave Geodetic Survey System (SHIRAN) Phase I System Analysis and Preliminary Design. ASD Technical Documentary Report ASD-TDR-62-872, Cubic Corp., June 1963 (Available from ASTIA AD-413-878).

4. Robinson, Gilbert G.; and Johnson, Norman S.: Subsystem Requirements for an Airborne Laboratory to Study Zero-Zero Landing Systems. Presented to Flight Mechanics Panel of AGARD (Munich, Germany), Oct. 12-14, 1964.

5. Develet, J. A., Jr.: Fundamental Accuracy Limitations in a Two-Way Coherent Doppler Measurement System. IRE Trans. Space Electronics and Telemetry, vol. SET-7, no. 3, Sept. 1961, pp. 80-85.

6. Shapiro, A. H.: Theoretical Error Analysis of the SCF Augmented Doppler Tracking System. Rep. SSD-TDR-63-339, Aerospace Corp., May 8, 1964.

7. Edson, W. A.: Noise in Oscillators. Proc. IRE, vol. 48, no. 8, Aug. 1960, pp. 1454-1466.

8. Baghdady, E. J.; Lincoln, R. N.; and Nelin, B. D.: Short-Term Frequency Stability: Characterization, Theory, and Measurement. Proc. IEEE, vol. 53, no. 7, July 1965, pp. 704-722.

9. Vessot, R.; Mueller, L.; and Vanier, J.: The Specification of Oscillator Characteristics from Measurements Made in the Frequency Domain. Proc. IEEE, vol. 54, no. 2, Feb. 1966, pp. 199-207.

10. Pratt, Harold J., Jr.: Propagation, Noise, and General Systems Considerations in Earth-Space Communications. IRE Trans. Comm. Systems, vol. CS-8, no. 4, Dec. 1960, pp. 214-221.

11. Churchill, Ruel V.: Complex Variables and Applications. McGraw-Hill Book Co., 1960, p. 166.

12. Gardner, Floyd M.: Phaselock Techniques. Ch. 2. John Wiley and Sons, Inc., 1966.

13. Berkowitz, Raymond S. (ed.): Modern Radar; Analysis, Evaluation and System Design. John Wiley and Sons, Inc., 1965, p. 12.

14. Millman, Jacob; and Taub, Herbert: Pulse, Digital and Switching Waveforms. McGraw-Hill Book Co., 1965, pp. 726-727.

15. Mechtly, E. A.: The International System of Units. NASA SP-7012, 1964, p. 5.

16. Dwight, Herbert B.: Tables of Integrals and Other Mathematical Data. Fourth Ed., MacMillan Co., 1961.

17. Schwartz, Mischa: Information, Transmission, Modulation, and Noise. McGraw-Hill Book Co., 1959, p. 207.

18. Jaffe, R.; Rechtin, E.: Design and Performance of Phase-Lock Circuits Capable of Near-Optimum Performance Over a Wide Range of Input Signal and Noise Levels. IRE Trans. Info. Theo., vol. IT-1, no. 1, March 1955, pp. 66-76.

19. Hodgman, Charles D. (ed.): Handbook of Chemistry and Physics, 42 Ed. The Chemical Rubber Publishing Co., Cleveland, 1960, p. 3086.

20. McCuskey, Sidney W.: Introduction to Celestial Mechanics. Addison-Wesley; Reading, Mass., 1963.

NASA-Langley, 1967 — 10 A-2662

"The aeronautical and space activities of the United States shall be conducted so as to contribute . . . to the expansion of human knowledge of phenomena in the atmosphere and space. The Administration shall provide for the widest practicable and appropriate dissemination of information concerning its activities and the results thereof."

—NATIONAL AERONAUTICS AND SPACE ACT OF 1958

NASA SCIENTIFIC AND TECHNICAL PUBLICATIONS

TECHNICAL REPORTS: Scientific and technical information considered important, complete, and a lasting contribution to existing knowledge.

TECHNICAL NOTES: Information less broad in scope but nevertheless of importance as a contribution to existing knowledge.

TECHNICAL MEMORANDUMS: Information receiving limited distribution because of preliminary data, security classification, or other reasons.

CONTRACTOR REPORTS: Scientific and technical information generated under a NASA contract or grant and considered an important contribution to existing knowledge.

TECHNICAL TRANSLATIONS: Information published in a foreign language considered to merit NASA distribution in English.

SPECIAL PUBLICATIONS: Information derived from or of value to NASA activities. Publications include conference proceedings, monographs, data compilations, handbooks, sourcebooks, and special bibliographies.

TECHNOLOGY UTILIZATION PUBLICATIONS: Information on technology used by NASA that may be of particular interest in commercial and other non-aerospace applications. Publications include Tech Briefs, Technology Utilization Reports and Notes, and Technology Surveys.

Details on the availability of these publications may be obtained from:

SCIENTIFIC AND TECHNICAL INFORMATION DIVISION

NATIONAL AERONAUTICS AND SPACE ADMINISTRATION

Washington, D.C. 20546